

A DNA-binding activity in BPV initiator protein E1 required for melting duplex *ori* DNA but not processive helicase activity initiated on partially single-stranded DNA

Cyril M. Sanders*

Institute for Cancer Studies, University of Sheffield, Beech Hill Rd, Sheffield, S10 2RX, UK

Received December 10, 2007; Revised January 14, 2008; Accepted January 22, 2008

ABSTRACT

The papillomavirus replication protein E1 assembles on the viral origin of replication (*ori*) as a series of complexes. It has been proposed that the *ori* DNA is first melted by a head-to-tail double trimer of E1 that evolves into two hexamers that encircle and unwind DNA bi-directionally. Here the role of a conserved lysine residue in the smaller tier or collar of the E1 helicase domain in *ori* processing is described. Unlike the residues of the AAA+ domain DNA-binding segments (β -hairpin and hydrophobic loop; larger tier), this residue functions in the initial melting of duplex *ori* DNA but not in the processive DNA unwinding of partially single-stranded test substrates. These data therefore define a new DNA-binding related activity in the E1 protein and demonstrate that separate functional elements for DNA melting and helicase activity can be distinguished. New insights into the mechanism of *ori* melting are elaborated, suggesting the coordinated involvement of rigid and flexible DNA-binding components in E1.

INTRODUCTION

The initiation of DNA replication begins with the recruitment of specific proteins to defined sequences and is followed by the melting of the origin (*ori*) of replication (1,2). How initiators melt DNA is poorly understood but protein-induced looping (3), wrapping (4–6) or encircling of the DNA can distort and melt DNA. Large T antigen (LTag) and E1, the initiator proteins of SV40 and papillomavirus respectively, both encircle DNA when melting it. The replication mechanisms of these viruses

have received much attention as their genomes are regulated like that of the mammalian host cells they infect, and because the papillomaviruses are important disease organisms in man. LTag and E1 both assemble as multi-protein complexes at their respective *oris* (7,8), and melt the DNA either side of their initiator-binding sites (9,10).

The bovine papillomavirus (BPV-1) replication initiation complex assembles in a stepwise fashion (8). E1 is first recruited as a dimer to two binding sites in *ori* by the viral transcription factor E2 (11–13). In a subsequent ATP-dependent reaction, E2 is displaced and more E1 molecules are recruited (14,15). The initial complex that forms is stable in the presence of ATP but does not melt the DNA (16). The sequence-specific DNA-binding domain (DBD) of E1 performs an essential function in this process, targeting E1 to a third and fourth binding site in the E1 recognition sequence (17). The next step in initiation is the transition from tetramer to double trimer (DT) with the concomitant melting of the *ori* DNA (18), and occupation of a fifth and sixth binding site by the E1 DBD. In a process so far unique to the DNA tumour viruses, the melted DNA then becomes the substrate upon which a replicative helicase forms from the *ori*-melting complex. The active form of the helicase is a hexamer and two hexamers unwind the DNA bi-directionally (19,20). Indeed, the concerted action of two hexameric helicases is not limited to replication, as two hexameric helicases also drive branch migration during recombination (21,22). This could suggest that the functioning of hexameric helicases in pairs is a more general phenomenon.

A mechanistic understanding of these processes has benefited from the determination of the three-dimensional crystal structures of the BPV-1 E1 DBD (23,24), fragments of an E1-E2 complex (25), and more recently the structure of the E1 helicase domain (26,27). Like the LTag helicase domain (28) the E1 helicase domain (HD, residues 299–605) assembles to form a hexamer

*To whom correspondence should be addressed. Tel: +44 114 2712482; Fax: +44 114 2713892; Email: c.m.sanders@sheffield.ac.uk

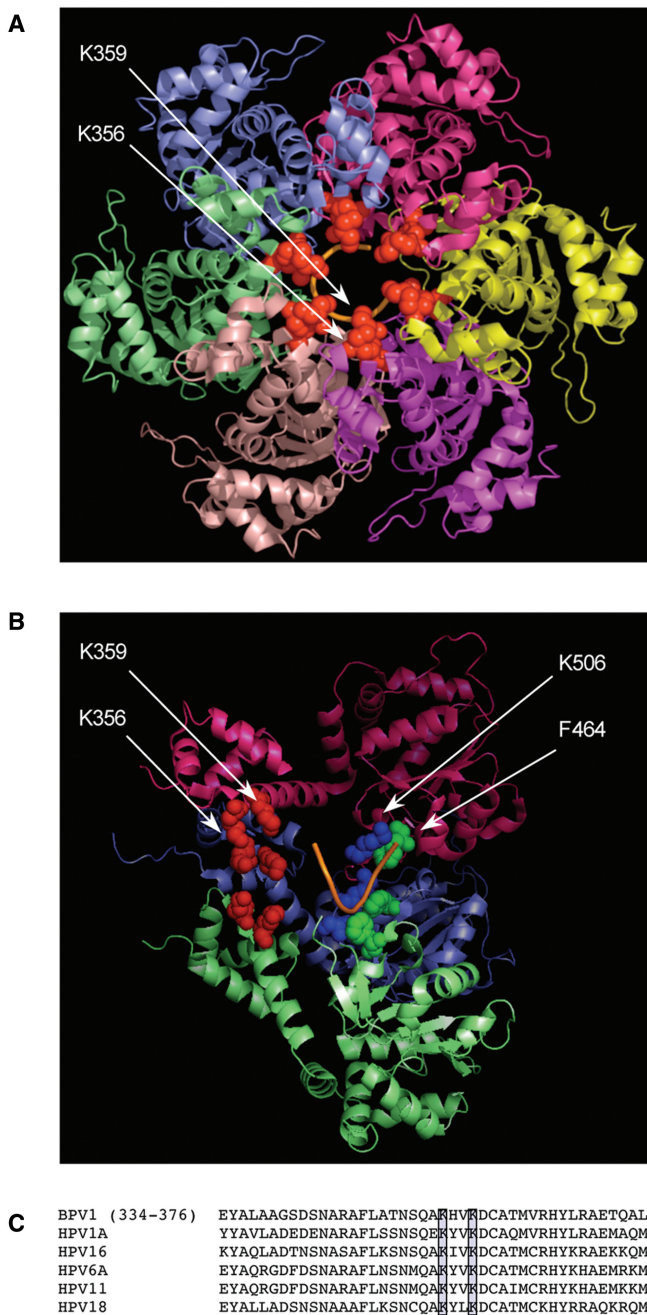


Figure 1. Conserved structural features of the E1 hexamer DNA-binding tunnel. (A) View of the E1/ADP/DNA complex [(26); pdb file 2GXA] from the collar domain through the DNA-binding tunnel. K356 and K359 are shown as red spheres in each subunit. The ssDNA backbone (T6) is shown in orange. (B) Rotation of the structure with three subunits removed through 90° to show the longitudinal position of residues. K356 and K359 are again shown as red spheres. K506 (β -hairpin, blue spheres) and F464 (hydrophobic loop, green spheres) in the AAA+ domain are also shown. (C) Alignment of papillomavirus E1 sequences with BPV E1 residues 334–376, generated with CLUSTAL W alignment software. Conserved lysines corresponding to BPV residues K356 and K359 are highlighted.

with a large and small tier (Figure 1). With and without co-factors and DNA the N-terminal domains of E1 HD (residues ~300–378) form a near symmetrical ring or ‘rigid collar’, while the ATPase or AAA+ domains (residues

379–605) are arranged asymmetrically (26,27). Two DNA-binding segments in the AAA+ domain have been identified; a β -hairpin (residues 505–509) and a ‘hydrophobic loop’ (residues 457–467), that have functional equivalents in LTag (28,29). A conserved lysine and phenylalanine (K506 and F464 in BPV) are critical for both helicase activity and DNA melting (30). In the E1/ADP/DNA hexamer these residues form the principal contacts with ssDNA passing through a central tunnel, and follow a wave-like path correlating with ATP, ADP and apo-configurations of the nucleotide-binding sites at the subunit interfaces. Although these data illuminate an attractive mechanism for nucleotide-coupled ssDNA translocation through the helicase, models for DNA melting are fragmentary. Here I show that a conserved lysine residue, K356 in the E1 HD collar domain, that has its side chain exposed in the central tunnel of the E1 hexamer is important for the melting of duplex *ori* DNA but not processive DNA strand separation initiated on partially single-stranded DNA test substrates. These data suggest that the E1 HD collar and AAA+ domains both possess DNA-binding functions that act in concert when E1 melts *ori*. The propensity of the collar domains to form a symmetrical structure while the AAA+ domains are inherently flexible suggests a ‘clamp and twist’ mechanism for dsDNA remodelling by an E1-*ori* complex.

MATERIALS AND METHODS

Protein expression and purification

Mutagenesis was performed by overlapping primer extension and sequences verified in full (ABI; Core Genomics Facility, University of Sheffield). E1 proteins were purified as described previously (30), and concentrations determined by BioRad assay using BSA as a standard.

E1 DNA-binding reactions and gel-shift assays

The pUC plasmid construct (X/12) containing the BPV minimal origin sequence has been described previously (15). A 177 bp ³²P end-labelled product was generated by PCR with the primers 5'-GTAAAACGACGGCCAGT (upstream primer, labelled) and 5'-GGATAACAATTTCACACAGG (downstream) and gel purified. *Ori*-binding reactions (30 min incubation) were performed in 20 mM sodium phosphate (pH 7.2), 135 mM NaCl, 10% v/v glycerol, 0.1% v/v NP-40, 0.1 mg/ml BSA, 1 mM PMSF, 1 mM DTT and 125 pg/ μ l poly(dA-dT)_n, with 5 mM ATP/MgCl₂. Products were analysed on agarose/TAE gels following glutaraldehyde cross-linking (15). Imaging and quantification was achieved by phosphor-imaging (Fuji FLA3000, Image gauge V3.3 software).

Helicase assays

Helicase activity was determined by the ability of E1 proteins to displace a 70 bp ssDNA strand from a substrate with a 45 base 3' tail, as described previously (30). The substrate was generated by annealing and extending a ³²P end-labelled primer on a 115 bp ssDNA sequence. The reaction buffer was 20 mM HEPES-NaOH pH 7.5,

20 mM NaCl, 1 mM DTT, 1 mM ATP and 3 mM MgCl₂. Assays (20 µl) were performed at 22°C for 60 min and terminated by adjusting the reaction to 20 mM EDTA, 0.1% w/v SDS, 10% v/v glycerol and 0.13% w/v bromophenol blue. Products were resolved on 8% polyacrylamide gels (19:1) containing 0.05% w/v SDS. Imaging and quantification was as described above.

The fragment unwinding assay was performed with the 177 bp *ori* probe as substrate (0.1 nM), in the presence of 2.5 pg/µl RPA (31). The reaction buffer was 20 mM Tris-HCl, 10% v/v glycerol, 0.1% v/v NP-40, 0.1 mg/ml BSA, 1 mM PMSF, 1 mM DTT, 125 pg/µl poly(dA-dT)_n and 5 mM ATP/MgCl₂. Reactions were incubated for 1 h at 22°C and terminated by adding SDS to 0.1% w/v and proteinase K to 0.25 mg/ml. After a further 15 min incubation, products were resolved on 5% 80:1 acrylamide:bis-acrylamide gels with 0.25× TBE electrophoresis buffer, both containing 0.05% w/v SDS. Dried gels were phosphor-imaged as described above.

Potassium permanganate assay

Binding conditions (0.2 nM probe), were as described above. KMnO₄ modification was performed in the presence of 25 mM MgCl₂ as described previously (16,30). Modified DNA was recovered by phenol/chloroform extraction and ethanol precipitation prior to piperidine cleavage. Reaction products were resolved on an 8% urea-PAGE sequencing gel and dried gels visualised by phosphor-imaging.

Hydroxyl radical footprinting

The binding conditions (0.2 nM probe) were as described above, except that glycerol was omitted from the reaction. OH radical cleavage was performed according to the general guidelines of Dixon *et al.* (32). DNA cleavage was quenched by the addition of 0.5 vols 200 mM thiourea, 25% v/v glycerol, 2 mM EDTA, 2% w/v SDS and 20 µg glycogen carrier. Reactions were processed with proteinase K and phenol/chloroform extracted and ethanol precipitated for analysis on 8% urea-polyacrylamide gels, as above.

In vivo replication assays

Constructs for *in vivo* replication, pUC-*ori* X/12, pCGE2 and pCGE1 have been described previously (15,33). Mutants in pCGE1 were constructed by overlapping primer extension and insertion of an XmaI-SpeI fragment into the pCGE1 construct digested with the same enzymes. Insert sequences were verified in full. CHO K1 cells in six-well plates were transfected (1 µg pUC-*ori*, 0.1 µg pCGE2 and the indicated amounts of pCGE1 constructs), with Lipofectamine 2000, according to the manufacturers' instructions. For time points greater than 36 h, cells were trypsinised 24 h post-transfection and transferred to 9-cm dishes. DNA was extracted from the cells by a modified alkaline lysis procedure (33), and further processed with proteinase K, phenol/chloroform extraction and ethanol precipitation before digestion with RNase A, DpnI and HindIII. Products were resolved on 1% agarose gels and transferred to Hybond N+ membrane (GE Healthcare)

by standard capillary blotting methods, and hybridised with a pUC-*ori*-specific probe, in Rapid-Hyb buffer (GE Healthcare). Blots were visualised by phosphor-imaging.

In vitro replication assays

Cell-free extracts were prepared from FM3A cells as described previously (34). Reactions were performed in 20 mM HEPES-NaOH pH 7.5, 10 mM NaCl, 1 mM EDTA, 2 mM DTT, 0.1 mM PMSF, with 4 mM ATP, 0.2 mM each GTP, UTP and CTP, 0.1 mM each dATP, dGTP and dTTP, 0.01 mM dCTP, 7 mM MgCl₂ and 40 mM creatine phosphate. Reactions (25 µl) contained 5 µCi [α -³²P]-dCTP (3000 Ci/mmol), 0.4 µg creatine phosphokinase, 70 µg of poly-glutamic acid, 6–8 µl of cell extract, 50 ng of pUC-*ori* template and E1 proteins as indicated. After 90 min incubation (37°C) reactions were terminated by the addition of 170 µl of stop buffer (0.1 M Tris pH 7.4, 0.35 M Na acetate, 10 mM EDTA 0.5% w/v SDS), 4 µl of proteinase K and 1 µl of glycogen (20 mg/ml). After 30 min incubation at 37°C reactions were phenol/chloroform extracted, ethanol precipitated and resolved on 1% agarose gels for drying and phosphorimaging.

RESULTS

Conserved tunnel residues of the E1 helicase collar domain

Conserved amino acids in the β -hairpin and a hydrophobic loop in the E1 AAA+ domain are required for duplex origin DNA melting and helicase activity initiated on partially single-stranded DNA test substrates (30). Both of these structures project into the central tunnel formed by E1 hexamerisation and follow a wave-like trajectory along its longitudinal axis, contacting ssDNA directly in the E1/ADP/DNA crystal structure (26). Further inspection of this structure reveals two additional lysine residues in the smaller E1 HD N-terminal collar domain, K356 and K359, whose side chains also point directly into the tunnel (Figure 1A). Unlike the residues of the AAA+ domain DNA-binding sites, these amino acids do not follow a wave-like path but form a ring dictated by the near-symmetry of the collar domain (Figure 1A and B). Direct contacts of K356 or K359 with DNA were not observed in the E1/ADP/DNA crystal structure and no clear electron density corresponding to DNA was apparent in this domain (26). Alignment of papillomavirus E1 amino acid sequences reveals that lysine is highly conserved at positions analogous to BPV residues 356 and 359. With only one exception in all available sequences (glutamine), arginine is the only other amino acid frequently found at either position (Figure 1C).

Helicase activity of E1 collar domain mutants

Helicase activity of E1 collar domain mutants was assessed by measuring the displacement of a ³²P-labelled 70 base DNA strand annealed to a 115 base strand, forming a substrate with a 45 base 3' overhang (Figure 2). At the lowest concentration of protein tested (50 nM), the helicase activity of mutants K356A, K356E and K356Q

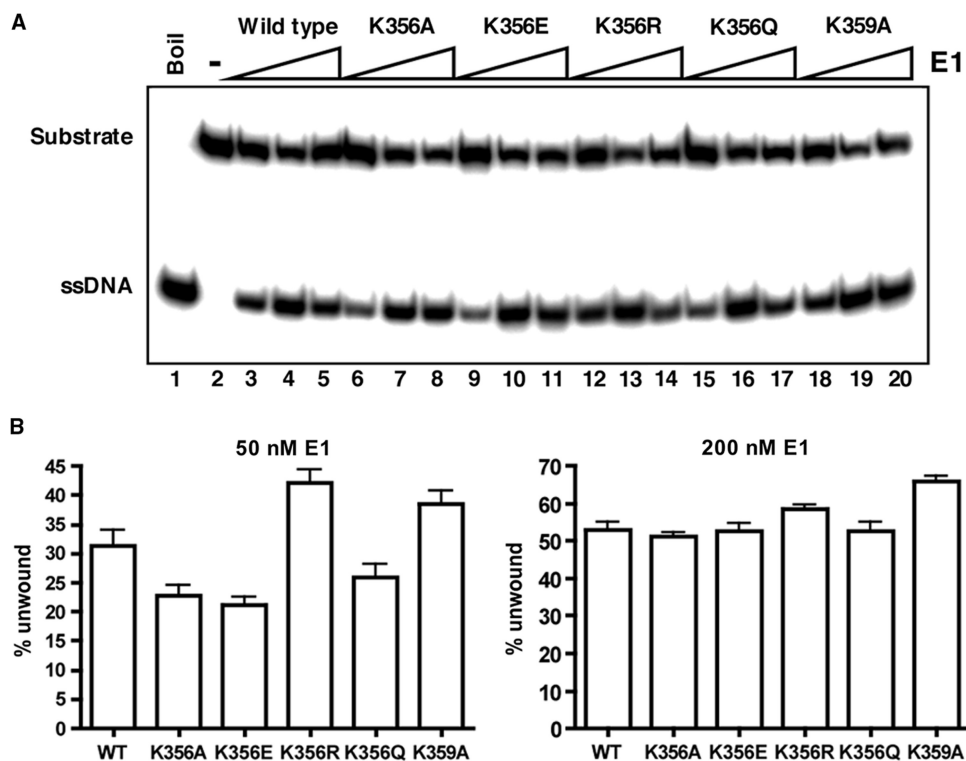


Figure 2. Helicase activity of E1 and collar domain mutants. (A) Representative data for E1 catalysed unwinding of a 70 bp ^{32}P -labelled duplex strand from a substrate with a 45 base 3' tail (50, 200 and 800 nM E1). Lane 1, boiled substrate, lane 2 no protein and lanes 3–20 E1 proteins as indicated. (B) Statistical data for unwinding reactions performed with 50 and 200 nM E1 proteins, generated from quantified phosphorimages.

was slightly lower than wild-type (reduced approximately 30% in the case of K356E), while the conservative substitution K356R and K359A appeared more active than wild-type. At 200 nM E1, the unwinding activity of wild-type E1 and all mutants (lanes 6–20) was similar (Figure 2B), with inhibition of the unwinding reaction at high protein concentrations. As has been shown previously, full-length E1 proteins with mutations in the AAA+ domain DNA-binding segments (K506 and F464), purified similarly, were inactive for unwinding (data not shown). Therefore, mutation of residues K356 and K359 does not impact significantly on E1 helicase activity initiated on partially single-stranded DNA test substrates.

Local *ori* melting requires a basic residue at position 356

Reactions with E1 proteins and an end-labelled *ori* probe were assembled in the presence of ATP and the potassium permanganate footprinting assay performed to measure DNA melting (Figure 3A) and the gel-shift assay to measure binding site occupancy (Figure 3B shown immediately below with corresponding reaction numbers). In the KMnO_4 assay, T residues in unwound DNA become hyper-reactive to oxidation and modified bases can be detected following cleavage with pipridine. As has been demonstrated previously (10,15), E1 *ori* melting is evident as thymidine cleavage products upstream and downstream of the E1-binding site (Figure 3A lanes 2–4; A/T-rich region and nucleotides 20, 26/27). Of the K356 mutants

tested, the conservative substitution K356R behaved like wild-type (lanes 11–13), while K356E failed to induce the extended permanganate hyper-reactivity over the A/T-rich region. Weak KMnO_4 reactivity was however apparent downstream of the E1-binding site at nucleotides 20, 26 and 27 (lanes 8–10). The extent of *ori* melting by K356Q (lanes 14–16) and K356A (lanes 5–7) was reduced compared to wild-type, with the K356A consistently more defective than the glutamine substitution. The *ori*-melting activity of K359A was similar to wild-type (lanes 17–19). The gel-shift analysis (Figure 3B) demonstrated that of all the mutant proteins only K356E showed a modest (less than twofold) decrease in dsDNA-binding activity, hence the defects in *ori* melting are not a result of a primary defect in E1-*ori* DNA binding. However, it is notable that only lower order complexes appear to be generated in the gel-shift for K356E (lanes 8–10), as judged by the mobility of gel-shift complexes compared to wild-type. These data therefore indicate that a basic residue at position 356 is required for efficient DNA melting, while the opposing charge (glutamate) is inhibitory.

Ori-DNA unwinding by E1 and collar domain mutants

The dsDNA fragment unwinding assay is a helicase assay that is dependent on, as a pre-requisite, all the initiator activities of E1. Wild-type E1 and mutants were tested for their ability to unwind a 177 bp *ori*-DNA substrate with one strand end-labelled, where substrate and ssDNA

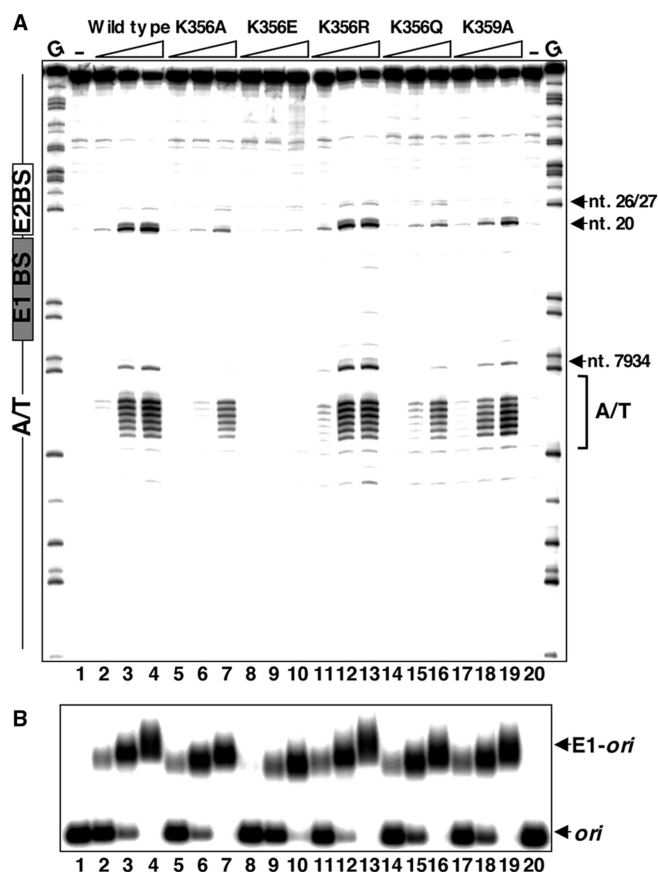


Figure 3. Initiator activity of E1 collar domain mutants. (A) Binding reactions were assembled with ATP, the 177 bp *ori* probe and E1 proteins (20, 40 and 80 nM). Reactions were processed to determine *ori*-melting (KMnO₄ assay, urea-PAGE gel above) and DNA-binding activity (gel-shift gel, below). On the urea-PAGE gel the position of *ori* DNA-binding sites and the A/T-rich region are indicated with reference to the G ladder (G), generated with DMS. Lanes 1 and 20 show the reactivity of free probe. (B) For each mutant, KMnO₄ reactivity can be compared at near complete probe binding determined by gel-shift analysis.

product were resolved by gel electrophoresis, following treatment of reactions with SDS and proteinase K. Figure 4A shows representative data and Figure 4B statistical data from three independent experiments. Figure 4A lane 1 is the substrate and lane 26 the substrate boiled. K356R (lanes 14–17) and K359A (lanes 22–25) had activities similar to wild-type E1 (lanes 2–5), while K356E was inactive (lanes 10–13). Substrate unwinding by mutant K356Q (lanes 18–21) was impaired but to a lesser extent than K356A (lanes 6–9). The fragment unwinding activities of the collar domain mutants therefore parallel the defects observed in the KMnO₄ DNA melting assay (Figure 3A). Since all mutants are capable of processive DNA unwinding, with similar activities at high protein concentrations, when unwinding is initiated directly from a substrate with an ssDNA tail (Figure 2), the fragment unwinding activities observed here are probably a measure of replication initiation. As none of the mutants have substantial defects in *ori* recognition, this most likely reflects a defect in *ori* melting.

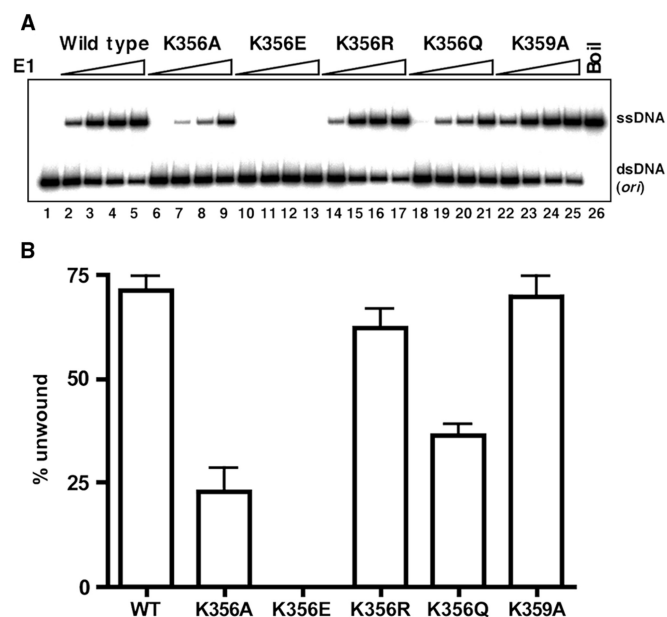


Figure 4. *Ori* fragment unwinding activity of E1 and mutants. (A) Unwinding of a 177 bp dsDNA *ori* substrate by wild-type E1 and mutants was measured by resolving substrate (lane 1) from ssDNA product (lane 26, boil) in a polyacrylamide gel, after treating reactions with SDS and proteinase K. E1 proteins (2.5, 5, 10 and 25 nM) were titrated in a low salt buffer as indicated. (B) Statistical data for fragment unwinding assays (25 nM protein, shown below), was generated from quantified phosphorimages.

Hydroxyl-radical footprinting of *ori* complexes

In the presence of ATP, E1 at low concentration binds to *ori* as a stable multimeric complex that does not melt the DNA. A distinct periodic hydroxyl-radical (OH) protection pattern is observed for this complex, closely resembling that observed for the complex first deposited on *ori* by E2 and E1 DNA binding in the absence of ATP. At higher concentrations of E1, with ATP, E1 melts DNA and an extended block OH protection appears over *ori*, correlating with the recruitment of more E1 to the DNA (16). Mutants in the DNA-binding segments of the E1 AAA+ domain that fail to melt *ori*, K506 and F464 of the β -hairpin and hydrophobic loop respectively, also generate only the periodic OH protection pattern in the presence of ATP (30). Failure to melt *ori* therefore appears to correlate with a failure in progressive E1 binding to *ori*. In Figure 5, wild-type E1 binding to *ori* at high concentrations in the presence of ATP generated an extended protection over *ori* (lanes 2–4), as previously observed. All mutants capable of DNA melting, even those with reduced activity (K356A and K356Q, Figure 3A), produced a protection pattern similar to wild-type. However, K356E (lanes 8–11) generated the periodic protection pattern that persisted even when the protein concentration exceeded that required for complete E1-binding site occupancy (lane 11). Therefore, the K356E mutant that is defective in *ori* melting is also defective in progressive E1 binding, like the K506 and F464 mutants of the AAA+ domain DNA-binding segments (30). These data demonstrate that DNA-binding functions residing

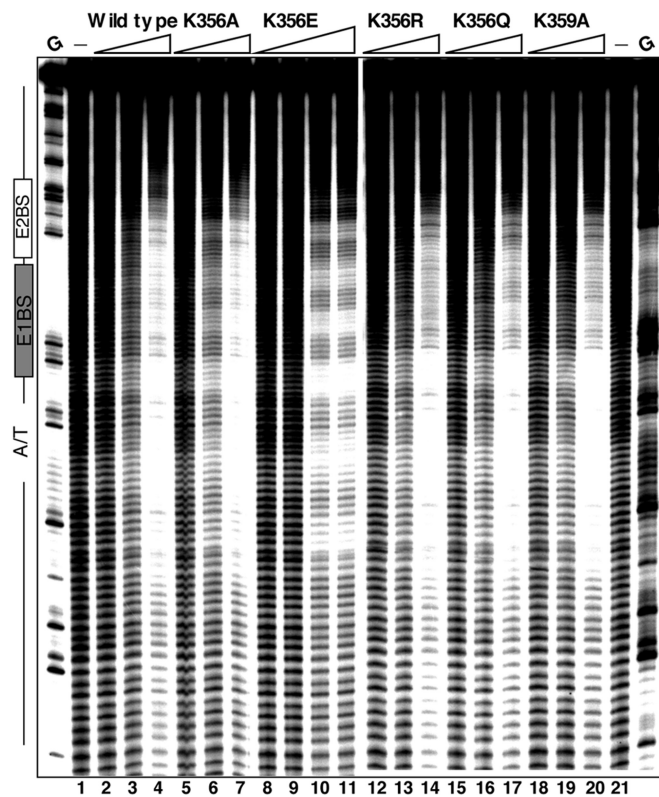


Figure 5. Hydroxyl radical protection of *ori* by wild-type E1 and collar domain mutants. Binding reactions were assembled in the absence of glycerol with a ^{32}P end-labelled *ori*-binding site probe and E1 titrated from 25, 50 and 100 nM, as indicated for each mutant. The titration for K356E was extended to 140 nM (lane 11). Reaction products were resolved on urea-PAGE sequencing gels. Lanes 1 and 21 show the OH reactivity of free probe.

in both the E1HD collar and AAA + domains cooperate to melt *ori*.

Replication activity of E1 collar domain mutants *in vivo* and *in vitro*

To test the replication activity of E1 collar domain mutants *in vivo*, CHO cells were co-transfected with E1 and E2 expression plasmids and a pUC-*ori* reporter plasmid, and DNA isolated for southern blot analysis at time intervals up to 72 h post-transfection. The BPV E2 transcription factor is absolutely required for E1-dependent replication *in vivo* (33). To detect replicated DNA only, DpnI was used to digest the un-replicated and methylated input bacterial plasmid. In Figure 6A, cells were co-transfected with fixed amounts of E2 expression vector and *ori* plasmid, and varying amounts of E1 expression constructs for DNA isolation after 48 h. The lowest levels of input wild-type E1 expression vector (250 ng per assay) supported replication (lane 1). Replication increased when cells were transfected with 1000 ng of E1 vector (lane 2), but 2500 ng per assay did not support more vigorous replication (lane 3). In the absence of E2, no replication activity was detected (lanes 19–21). For the collar domain mutants, the lowest concentration of E1 expression vector (250 ng) supported replication

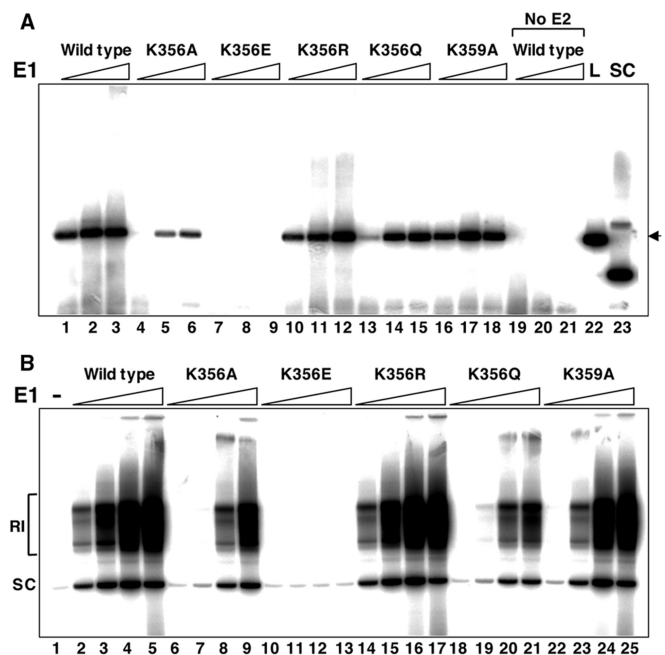


Figure 6. Replication *in vivo* and *in vitro*. (A) *In vivo* replication. CHO cells were co-transfected with an *ori*-plasmid (1000 ng) and expression constructs for E2 (100 ng) and wild-type E1/E1 mutants (250, 1000 and 2500 ng), as indicated. Plasmid DNA was isolated by alkaline lysis 48 h post-transfection and digested with HindIII to linearise the plasmid and DpnI to digest un-replicated and methylated input plasmid. Replicated DNA was detected by southern blotting and hybridisation with a ^{32}P -labelled *ori*-plasmid probe (lanes 22 and 23, 10 ng each linearised (L) and supercoiled (SC) *ori* plasmid). E1 collar domain mutants supported DNA replication at levels paralleling those of the *in vitro* initiation (DNA melting) assays. (B) Replication *in vitro*. Reactions (25 μl) were assembled with a cell-free protein extract from FM3A cells supplemented with the precursors of DNA synthesis, pUC-*ori* plasmid (2 ng/ μl) and the indicated E1 proteins (2, 4, 8 and 16 ng/ μl). Replication products labelled with α - ^{32}P dCTP were resolved in agarose gels and detected by phosphorimaging. Supercoiled product (SC) and replication intermediates (RI) are indicated. Lane 1 shows the background incorporation of radiolabel in the absence of any viral initiator protein.

at levels that directly paralleled their initiator activities in the biochemical assays described above: K356R and K359A supported replication at similar levels to wild-type E1 (lanes 10 and 16 compared to 1), the activities of K356A and K356Q were reduced (K356A to a greater extent than K356Q; lanes 4 and 13 compared to 1), and K356E was completely inactive (lane 7). With increasing concentration of expression construct, this trend was maintained and no replication was detected for K356E, even with the highest amount of expression vector tested (lanes 7–9). Similar results were obtained at earlier and later times (36 and 72 h post-transfection, data not shown).

The *in vitro* replication activity of E1 and mutant proteins was tested in a mammalian cell-free protein extract supplemented with *ori*-plasmid and the precursors of DNA synthesis (34). Replication products labelled with α - ^{32}P dCTP were resolved in agarose gels and visualised by phosphor-imaging (Figure 6B). Increasing concentrations of wild-type E1 promoted increasing levels of DNA synthesis (lanes 2–5). K356R and K359A (lanes 14–17 and 22–25) supported DNA synthesis at similar levels to

wild-type, although the lower concentrations of K359A (2 and 4 ng/ μ l, lanes 22 and 23) were less efficient than the corresponding concentrations of wild-type E1 and K356R (lanes 2 and 3 and 14 and 15). The replication activity of K356A (lanes 6–9) and K356Q (lanes 18–21) were both reduced compared to wild-type E1, with K356Q more efficient at promoting DNA synthesis at lower protein levels. K356E was completely inactive for replication (lanes 10–13). The replication activities of E1 collar domain mutants *in vivo* and *in vitro* therefore observe the same general trends, supporting the notion that a critical DNA-binding function resides in this domain.

DISCUSSION

Binding of E1 to DNA during initiator complex assembly has been explained in terms of the sequential pairwise recognition by the E1 sequence-specific DBD of six nested binding sites within the E1 recognition sequence (17). The initial recruitment of two E1 monomers to two E1-binding sites requires the viral transcription factor E2 that is displaced upon binding of E1 to additional sites (15). This E1-*ori* complex that forms is stable, but does not effectively generate the permanganate hyper-reactivity over the A/T-rich region (16). Progression to a double-trimer (DT) and melting of *ori* are co-ordinated events requiring the DNA-binding segments of the E1 ATPase/AAA+ portion of the E1HD (18,30). The data presented here demonstrate the existence of an additional DNA-binding function in the collar domain of the E1 HD entailing residue K356 that is also required for *ori* melting. The analysis performed *in vivo* and *in vitro* under physiologically relevant conditions, i.e. the presence of ATP, revealed stalling of E1-*ori* complex formation for the mutant K356E at the level of an E1-*ori* pre-initiation complex.

Nature of the E1-*ori* pre-initiation complex

Extensive high-resolution hydroxyl radical footprinting experiments have been performed with the E1 DBD and E1/E1E2 pre-initiation complexes. The periodic OH protection pattern observed for the E1-*ori* pre-initiation complex generated from E1E2-*ori* (16), closely resembles that of the E1-*ori* complex that forms without nucleotide co-factors (30,35), and for mutants in the E1HD DNA-binding domains [K356E, Figure 4 and the AAA+ domain β -hairpin (K506) and hydrophobic loop (F464), (30)]. In each case, protection over the E1 recognition motif is consistent with a tetramer of E1-binding sites 1–4 (of six) via the sequence-specific DBD (17), with the additional flanking protections generated by the non-specific DNA-binding segments of the E1 HD (36). The periodic nature of this OH footprinting pattern and the crystal structure of an E1 DBD tetramer bound to DNA (24) both indicate that encircling of the DNA is incomplete at this stage. However, structural changes in the template have begun. Distortions of the DNA helix are apparent in the E1-DNA co-crystal structure and limited KMnO₄ hyper-reactivity is induced by E1-*ori* formed without nucleotide cofactors (17). Permanganate

hyper-reactive sites are observed at nucleotide 7934, between the A/T-rich region and E1 recognition motif, and within the downstream E2BS. The latter are also induced by the HD collar and AAA+ domain DNA-binding mutants, particularly at nucleotide 20 but also 26 and 27 [Figure 3 and (30)]. Thus limited structural distortion of *ori* is a feature shared between the tetrameric pre-initiation complexes that can form under various conditions (directly from E1E2-*ori*, or without nucleotide cofactor) and with various mutants in the HD non-specific DNA-binding segments.

Nature of the collar domain DNA-binding function

Oligomerisation and encircling of ds- and ssDNA by E1-*ori* melting and helicase complexes is a feature associated with their respective activities. Subunit interactions are thus critical components of these DNA-binding assemblies. The data presented here demonstrate a role for K356 in dsDNA binding and melting. Unlike the previously characterised mutants in the AAA+ domain DNA-binding segments [K506 and F464 (30)], the DNA-binding defects of the K356 mutants do not correlate also with incapacitating defects in helicase activity (Figure 2). The mutant K356E demonstrated a modest (\sim twofold) decrease in dsDNA-binding activity, while K356A and K356Q bound the *ori* probe as effectively as wild-type (Figures 3 and 4). This suggests a role for K356 in forming a DNA-binding site, most likely through electrostatic interactions with the DNA, as highlighted by the severity of the K356E defect in DNA melting. It is possible that the non-conservative K356 mutations also affect the oligomerisation of E1 required to assemble the DNA-binding function. The observation that K356A, K356E and K356Q all have slightly reduced helicase activities compared to wild-type at low E1 concentrations (Figure 2B; \sim 30% maximum measured at 50 nM E1), may indicate a minor impairment in monomer–monomer interactions. However, it should be noted that these defects are not commensurate with the defects in duplex DNA melting, particularly for K356E that completely fails to melt double-stranded *ori* DNA. Also, the K356 side chain points directly into the central tunnel generated by E1 hexamerisation and does not appear to mediate any principal monomer–monomer contacts. More importantly, K356E and K356A have very similar helicase activities (Figure 2) but significantly different dsDNA-binding properties: K356E appears to form lower order complexes in the gel-shift assay shown in Figure 3B, even at high protein concentrations, generates a periodic OH footprinting pattern and completely fails to melt duplex *ori* DNA. On the other hand for K356A (and also K356Q), quantitative and qualitative defects in dsDNA binding are hard to discern by footprinting and gel-shift analysis, yet the defects in DNA melting are significant. Together, these observations are more readily reconcilable with a direct interaction of the K356 side chain with DNA during duplex opening, rather than a definitive contribution to monomer–monomer interactions and oligomerisation.

It is possible that residues in the collar domain other than K356 also contribute to DNA binding, although the data rule out the conserved lysine at position 359. All non-conservative K356 mutations tested showed a partial (K356A and K356Q) or complete (K356E) inability to melt *ori* over the A/T-rich region (Figure 3). However, only K356E generated the periodic OH protection pattern associated with the tetrameric pre-initiation complex at high protein concentrations, while all other mutants protected the DNA like wild-type. The similar OH protection patterns (absence of a partial or mixed footprint) would argue that the composition of all complexes that melt DNA is similar i.e. the DT forms. This would allow consideration of the melting activity of mutants in terms of specific activity, with various determinants contributing incrementally to generation of a stable unwound structure.

Amino-acid sequence comparisons with LTag do not readily reveal a potential functional equivalent of K356 alluding to a similar DNA-binding function in the collar domain of this protein. However, the sequences align poorly in this region and the three-dimensional arrangement of the LTag collar domain is different to E1 (27,28). None the less, the inner tunnel of the LTag hexamer is highly positively charged, indicating a likely contribution to the ss- and dsDNA-binding functions of LTag complexes.

Implications for the mechanism of *ori* melting

DNA-binding elements residing in three separate domains of E1 (DBD, collar and AAA+ domains) cooperate to melt *ori*, but exactly how this occurs upon DT formation is unclear. In the hexameric E1 helicase structures (26,27) the domains of the collar adopt a symmetrical conformation while the AAA+ domains are arranged asymmetrically. Rotation of the AAA+ domains by up to 14° result in positional deviations of up to 7.5 Å, and this flexibility appears to be an intrinsic feature of E1 assembly (27). There are no structures available for the E1 DT, but the requirement for a nucleotide (ATP or ADP *in vitro*) in stabilising the DT complex suggests intimate contacts between subunits. It is possible that the collar domains of the E1HD adopt a symmetrical configuration, while the AAA+ domain DNA-binding segments assemble asymmetrically, tracking the DNA bases along a helical trajectory as in the E1/ADP/DNA hexamer. As such, the DNA-binding modes of the HD collar and sequence-specific DBD could be viewed as a fixed clamp, while the flexible AAA+ domains are free to rotate. A rotational movement of the AAA+ domain, stabilised by nucleotide binding, may then untwist the DNA where extended permanganate hypersensitivity is measured (Figure 7). Further evaluation of the mechanism should be made possible with the new mutants described here.

ACKNOWLEDGEMENTS

This work was supported by Yorkshire Cancer Research grant S284. I thank Guanhua Yan for technical assistance in protein purification and Janet White for assistance with cell culture. Fred Antson and Oleg Kovalevskiy are

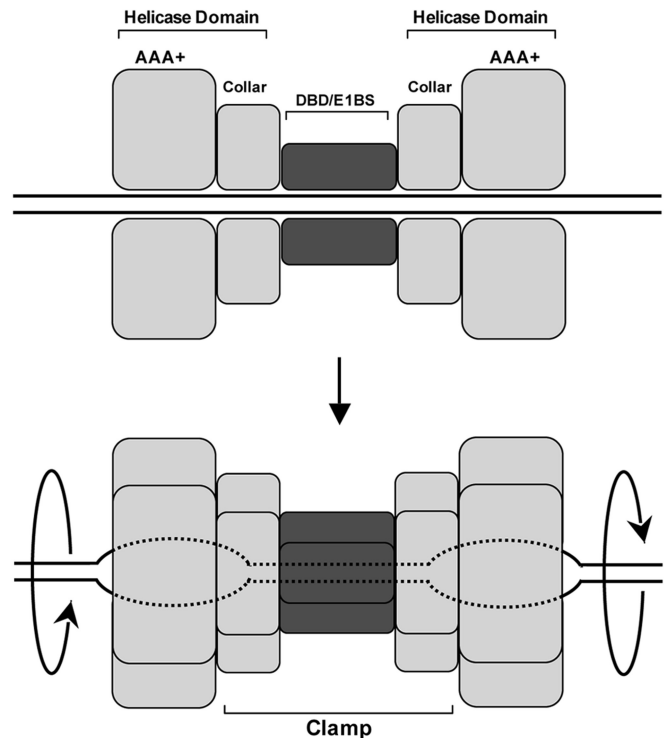


Figure 7. Proposed mechanism for melting of the BPV origin of replication. The DT *ori* melting complex is derived from a tetrameric pre-initiation complex. Three separate DNA-binding modules are required for melting: The sequence-specific DBD bound to the E1BS and binding sites in the collar and AAA+ portions of the helicase domain. On the basis of the rigid nature of the collar and DBD modules, these are proposed to form a clamp on the DNA about which rotation of the AAA+ domain induce untwisting of the DNA. A bound nucleotide (ATP or ADP) stabilises the unwound configuration.

thanked for useful discussion, and Mark Meuth, James Chong and Jon Sayers for critical reading of the manuscript. Funding to pay the Open Access publication charges for the article was provided by Yorkshire Cancer Research.

Conflict of interest statement. None declared.

REFERENCES

- Brush,G.S. and Kelly,T.J. (1996) Mechanisms for replicating DNA. In DePamphilis,M.L. (ed.), *DNA Replication in Eukaryotic Cells*, Cold Spring Harbor Laboratory Press, NY, USA, pp. 1–43.
- Mott,M.L. and Berger,J.M. (2007) DNA replication initiation: mechanisms and regulation in bacteria. *Nat. Rev. Microbiol.*, **5**, 343–354.
- Koff,A., Schwedes,J.F. and Tegtmeyer,P. (1991) Herpes simplex virus origin-binding protein (UL9) loops and distorts the viral replication origin. *J. Virol.*, **65**, 3284–3292.
- Fuller,R.S., Funnell,B.E. and Kornberg,A. (1984) The dnaA protein complex with the *E. coli* chromosomal replication origin (*oriC*) and other DNA sites. *Cell*, **38**, 889–900.
- Zahn,K. and Blattner,F.R. (1985) Binding and bending of the lambda replication origin by the phage O protein. *EMBO J.*, **13**, 3605–3616.
- Bramhill,D. and Kornberg,A. (1988) Duplex opening by dnaA protein at novel sequences in initiation of replication at the origin of the *E. coli* chromosome. *Cell*, **52**, 743–755.

7. Fanning,E. and Knippers,R. (1992) Structure and function of simian virus 40 large tumour antigen. *Annu. Rev. Biochem.*, **61**, 33–85.
8. Stenlund,A. (2003) Initiation of DNA replication: lessons from viral initiator proteins. *Nat. Rev. Mol. Cell Biol.*, **4**, 777–785.
9. Borowiec,J.A. and Hurwitz,J. (1988) Localised melting and structural changes in the SV40 origin of replication induced by T-antigen. *EMBO J.*, **7**, 3149–3158.
10. Gillette,T.G., Lusky,M. and Borowiec,J.A. (1994) Induction of structural changes in the bovine papillomavirus type 1 origin of replication by the viral E1 and E2 proteins. *Proc. Natl Acad. Sci. USA*, **91**, 8846–8850.
11. Lusky,M., Hurwitz,J. and Seo,Y.-S. (1993) Cooperative assembly of the bovine papilloma virus E1 and E2 proteins on the replication origin requires an intact E2 binding site. *J. Biol. Chem.*, **268**, 15795–15803.
12. Chen,G. and Stenlund,A. (1998) Characterisation of the DNA-binding domain of the bovine papillomavirus replication initiator E1. *J. Virol.*, **72**, 2567–2576.
13. Sanders,C.M. and Stenlund,A. (2001) Mechanism and requirements for bovine papillomavirus, type 1, E1 initiator complex assembly promoted by the E2 transcription factor bound to distal sites. *J. Biol. Chem.*, **276**, 23689–23699.
14. Lusky,M., Hurwitz,J. and Seo,Y.-S. (1994) The bovine papillomavirus E2 protein modulates the assembly of but is not stably maintained in a replication-competent multimeric E1-replication origin complex. *Proc. Natl Acad. Sci. USA*, **91**, 8895–8899.
15. Sanders,C.M. and Stenlund,A. (1998) Recruitment and loading of the E1 initiator protein: an ATP-dependent process catalysed by a transcription factor. *EMBO J.*, **17**, 7044–7055.
16. Sanders,C.M. and Stenlund,A. (2000) Transcription factor dependent-loading of the E1 initiator reveals modular assembly of the papillomavirus origin melting complex. *J. Biol. Chem.*, **275**, 3522–3524.
17. Chen,G. and Stenlund,A. (2002) Sequential and ordered assembly of E1 initiator complexes on the papillomavirus origin of DNA replication generate progressive structural changes related to *ori* melting. *Mol. Cell Biol.*, **22**, 7712–7720.
18. Schuck,S. and Stenlund,A. (2005) Assembly of a double hexameric helicase. *Mol. Cell*, **20**, 377–389.
19. Parsons,R., Stenger,J.E., Ray,S., Welker,R., Anderson,M.E. and Tegtmeyer,P. (1991) Cooperative assembly of simian virus 40 T-antigen hexamers on functional halves of the replication origin. *J. Virol.*, **65**, 2798–2806.
20. Sedman,J. and Stenlund,A. (1998) The papillomavirus E1 protein forms a DNA-dependent hexameric complex with ATPase and DNA helicase activities. *J. Virol.*, **72**, 6893–6897.
21. Parsons,C.A., Stasiak,A., Bennett,R.J. and West,S.C. (1995) Structure of a multisubunit complex that promotes DNA branch migration. *Nature*, **374**, 375–378.
22. Sharples,G.J., Ingleston,S.M. and Lloyd,R.G. (1999) Holliday junction processing in bacteria: insights from the evolutionary conservation of RuvABC, RecG, and RusA. *J. Bacteriol.*, **181**, 5543–5550.
23. Enemark,E.J., Chen,G., Vaughn,D.E., Stenlund,A. and Joshua-Tor,L. (2000) Crystal structure of the DNA binding domain of the replication initiation protein E1 from papillomavirus. *Mol. Cell*, **6**, 149–158.
24. Enemark,E.J., Chen,G., Vaughn,D.E., Stenlund,A. and Joshua-Tor,L. (2002) Crystal structure of two intermediates in the assembly of the papillomavirus replication initiation complex. *EMBO J.*, **21**, 1478–1496.
25. Abbate,E.A., Berger,J.M. and Botchan,M.R. (2004) The X-ray structure of the papillomavirus helicase in complex with its molecular matchmaker E2. *Genes Dev.*, **18**, 1981–1996.
26. Enemark,E.J. and Joshua-Tor,L. (2006) Mechanism of DNA translocation in a replicative hexameric helicase. *Nature*, **442**, 270–275.
27. Sanders,C.M., Kovalevskiy,O.V., Sizov,D., Lebedev,A.A., Isupov,M.N. and Antson,A.A. (2007) Papillomavirus E1 helicase maintains an asymmetric state in the absence of DNA and nucleotide cofactors. *Nucleic Acids Res.*, **35**, 6451–6457.
28. Li,D., Zhao,R., Lilyestrom,W., Gai,D., Zhang,R., DeCaprio,J.A., Fanning,E., Joachimiak,A., Szakonyi,G. and Chen,X.S. (2003) Structure of the replicative helicase of the oncoprotein SV40 large tumour antigen. *Nature*, **423**, 512–518.
29. Shen,J., Gai,D., Patrick,A., Greenleaf,W.B. and Chen,X. (2005) The roles of the residues on the channel β -hairpin and loop structures of simian virus 40 hexameric helicase. *Proc. Natl Acad. Sci. USA*, **102**, 11248–11253.
30. Castella,S., Bingham,G. and Sanders,C. (2006) Common determinants in DNA melting and helicase catalysed DNA unwinding by papillomavirus replication protein E1. *Nucleic Acids Res.*, **34**, 3008–3019.
31. Leigh,A.H., Umbricht,C.B. and Wold,M.S. (1994) Recombinant replication protein A: expression, complex formation, and functional characterization. *J. Biol. Chem.*, **269**, 11121–11132.
32. Dixon,W.J., Hayes,J.J., Levin,J.R., Weidner,M.F., Dombroski,B.A. and Tullius,T.D. (1991) Hydroxyl radical footprinting. *Methods Enzymol.*, **208**, 147–169.
33. Ustav,M. and Stenlund,A. (1991) Transient replication of BPV-1 requires two viral polypeptides encoded by the E1 and E2 open reading frames. *EMBO J.*, **10**, 449–457.
34. Yang,L., Li,R., Mohr,I.J., Clark,R. and Botchan,M.R. (1991) Activation of BPV-1 replication in vitro by the transcription factor E2. *Nature*, **353**, 628–632.
35. Sedman,J. and Stenlund,A. (1996) The initiator protein E1 binds to the bovine papillomavirus origin of replication as a trimeric ring-like structure. *EMBO J.*, **15**, 5085–5092.
36. Stenlund,A. (2003) E1 initiator DNA binding specificity is unmasked by selective inhibition of non-specific DNA binding. *EMBO J.*, **22**, 954–963.